Nanotechnology

PAPER

Electrically controllable terahertz square-loop metamaterial based on VO_2 thin film

To cite this article: Jun-Hwan Shin *et al* 2016 *Nanotechnology* **27** 195202

IOP Publishing Nanotechnology
Nanotechnology 27 (2016) 195202 (8pp) doi:10.1088/0957-4484/27/19/195202

Electrically controllable terahertz square-loop metamaterial based on VO_2 thin film

Jun-Hwan Shin[1,2], Kyung Hyun Park[1,2] and Han-Cheol Ryu[3]

[1] THz Photonics Creative Research Center, Electronics and Telecommunications Research Institute, 218 Gajeong-ro, Yuseong-gu, Daejeon 305-700, Korea
[2] School of Advanced Device Technology, University of Science & Technology, 217 Gajeong-ro, Yuseong-gu, Daejeon 305-350, Korea
[3] Department of Car Mechatronics, Sahmyook University, Seoul 139-742, Korea

E-mail: khp@etri.re.kr and hcryu@syu.ac.kr

Received 19 October 2015, revised 11 February 2016
Accepted for publication 8 March 2016
Published 4 April 2016

Abstract
An electrically controllable square-loop metamaterial based on vanadium dioxide (VO_2) thin film was proposed in the terahertz frequency regime. The square-loop shaped metamaterial was adopted to perform roles not only as a resonator but also as a micro-heater for the electrical control of the VO_2. A dual-resonant square-loop structure was designed to realize band-pass characteristics in the desired frequency band. The measured *Q*-factors of the basic and scaled-down metamaterials fabricated on VO_2 thin films were 2.22 and 1.61 at the center frequencies of 0.44 and 1.14 THz in the passbands, respectively. The transmittances of the proposed metamaterial were successfully controlled by applying a bias voltage without an external heater. The measured transmittance on–off ratios of the metamaterials were over 40 at the center frequencies in the passbands. In the future, electrically controllable terahertz metamaterial based on VO_2 metamaterial could be employed as high-performance active filters or sensors.

Keywords: terahertz wave, metamaterial, spectroscopy, vanadium dioxide, phase transition, microheater

(Some figures may appear in colour only in the online journal)

1. Introduction

Terahertz (THz) technology has received considerable interest because of its potential in a wide variety of applications such as wireless communication, spectroscopy, imaging, and sensing [1–3]. In the past couple of decades, cost-effective and compact THz sources and detectors have been intensively developed to use the THz wave in industrial applications [4–7]. For more practical THz applications, various active and passive devices such as THz filters, modulators, phase shifters, switches, and mirrors must be developed. However, the development of THz devices is delayed because the electromagnetic properties of most natural materials are not suitable to be used in the THz frequency range.

In recent years, metamaterials have attracted significant attention owing to their unique responses for manipulating electromagnetic resonances that are not usually found in natural materials. The response of metamaterials to electromagnetic waves is determined by the structure of metallic resonators with periodic patterns whose unit cell is smaller than the wavelength of the wave. The resonances of the metamaterials are characterized by both LC resonance of the unit cell and the periodicity of the structures [8]. The controllable resonances of the artificially engineered metamaterials can offer opportunities to realize novel THz devices for a wide variety of THz applications [9–12]. Numerous research studies on the realization of tunable characteristics for THz metamaterials have been reported by using semiconductors, graphene, and tunable functional materials [13–16]. Tunable metamaterials based on functional materials—especially vanadium dioxide (VO_2), which has reversible switching physical properties caused by insulator-to-metal transition at critical temperature 340 K—present one promising approach to spatially manipulate the THz wave thanks to easy fabrication and high tunability. Several studies have researched tunable THz metamaterials based on the phase

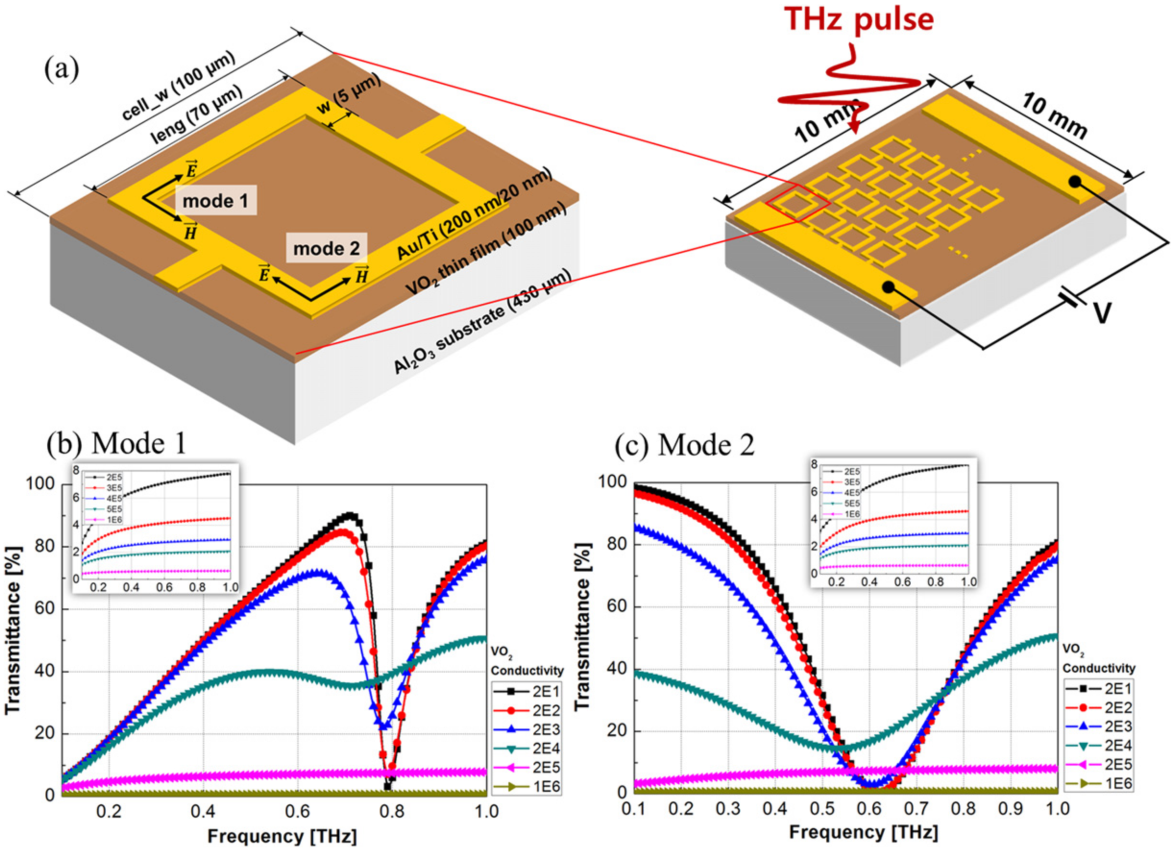

Figure 1. Simulation results for single-resonant square-loop metamaterial (SSLM) (a) schematics of the unit cell and the measured device, (b) transmittances in mode 1 and (c) in mode 2. (Insets of figures 1(b) and (c): detailed result for the conductivity in the range of 2×10^5–1×10^6).

transition of VO_2 by applying temperature, THz-field, or light [17–20]. However, these methods require external devices such as a heater or a source of THz wave or light; the external devices cause these THz tunable devices to be expensive and bulky. Thus, the electrical control for the phase transition of VO_2 is preferred for practical applications [21]. In addition, it is very important to design the tunable THz metamaterial based on VO_2 to be used in the desired THz frequency range; the design of the metamaterial for the operation in the specific frequency can enlarge its application fields.

In this paper, an electrically controllable THz square-loop metamaterial based on VO_2 thin film is presented. The dual-resonant square-loop metamaterial (DRSLM) is designed to have band-pass characteristics in the desired frequency range and also works as a micro-heater for the control of the conductivity on the VO_2 thin film. The designed and fabricated THz metamaterial based on VO_2 thin film was successfully controlled by a bias voltage without external sources.

2. Design and fabrication

Instead of a split-ring resonator, a closed loop-shaped resonator was adopted as a unit cell of the metamaterial to effectively increase the temperature of the VO_2 thin film by applying a bias voltage [22]. A bias line was attached to the two sides of the square-loop facing each other as shown in figure 1(a). The bias voltage applied to the bias line can generate the uniform current flowing through the whole metamaterial; the flowing current through the metamaterial could heat up the temperature of the VO_2 thin film by current induced Joule heating effect in metal structure. Thus, the adopted square-loop metamaterial can function not only as a resonator but also as a micro-heater. The width of the unit cell (*cell_w*) was 100 μm, the length of the square-loop (*leng*) was 70 μm, and the width of the metal line (w) was 5 μm. The square-loop of metamaterial was simulated using electromagnetic simulator HFSS with varying VO_2 conductivity from 20 to 1×10^6 S m^{-1} which values were confirmed by measurements as shown in figure 4(b). The thickness of the VO_2 thin film was set to 100 nm. The proposed metamaterial has different transmission characteristics according to the polarization state of the incident THz electric field. As shown in figure 1(a), mode 1 means the polarization of the electric field is parallel to the bias line; mode 2 means polarization is perpendicular to the line. The transmittances of a single-resonant square-loop metamaterial (SSLM) are plotted as a function of VO_2 conductivity in figure 1(b) (mode 1) and figure 1(c) (mode 2). The insets in figures 1(b) and (c) show the transmittances according to the varying VO_2 conductivity from 2×10^5 to 1×10^6 S m^{-1}. In figure 1(b), there were abrupt changes of THz wave transmittance in the frequency

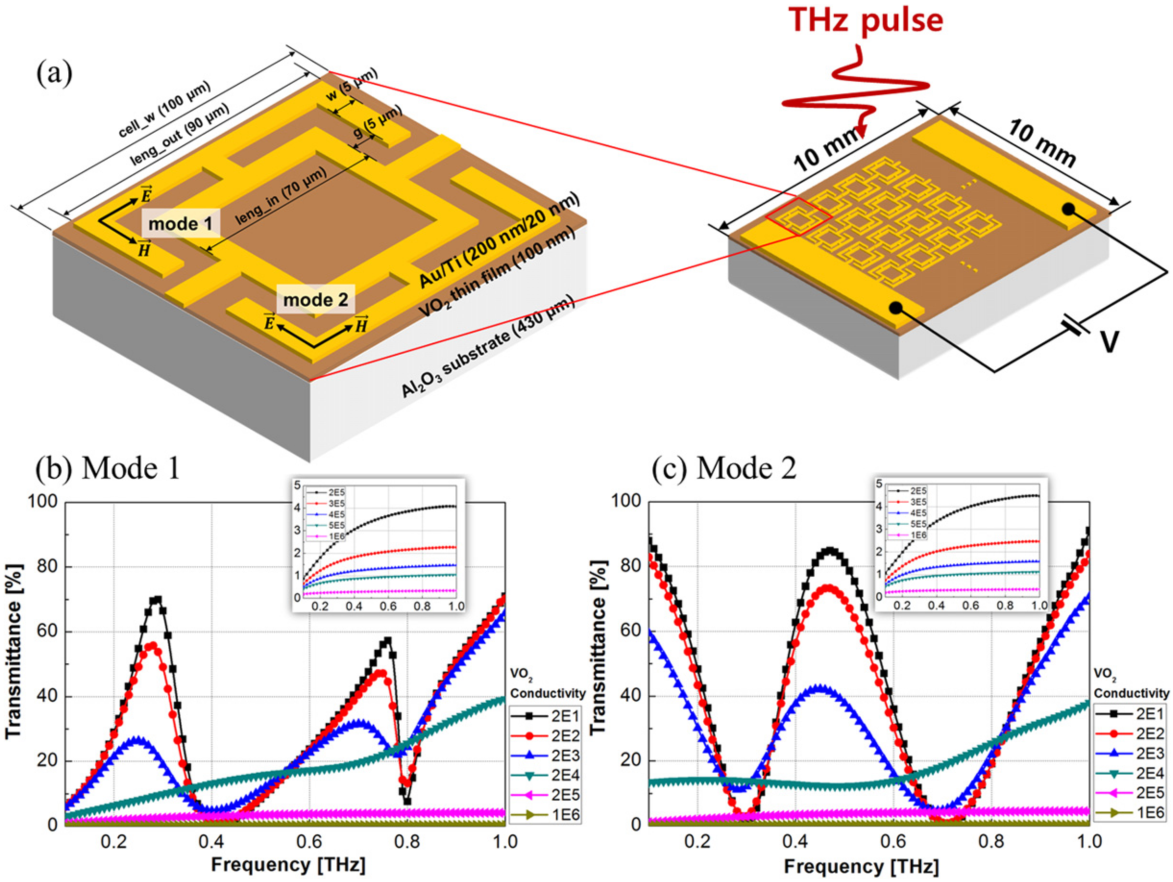

Figure 2. Simulation results for dual-resonant square-loop metamaterial (DSLM) (a) schematics of the unit cell and the measured device, (b) transmittances in mode 1 and (c) in mode 2. (Insets of figures 2(b) and (c): detailed result for the conductivity in the range of 2×10^5–1×10^6).

range between 0.7 and 0.8 THz. The transmittance characteristics of the SSLM operating in mode 2, as shown in figure 1(c), were more stable than those of the SSLM in mode 1. The resonance frequency of the SSLM in mode 2 was near 0.62 THz. As the VO_2 conductivity increased, the resonance of the SSLM was redshifted and its strength was weakened because of the increase in effective permittivity and degradation of the *Q*-factor, respectively.

A DSLM was proposed to realize band-pass characteristics in the specific frequency band. The schematic and transmittances of the DSLM operating in modes 1 and 2 are shown in figure 2. The size of the unit cell and the dimension of the basic square-loop structure inside the DSLM are the same as those of the SSLM—i.e., $cell_w = 100\ \mu$m, $leng_in = 70\ \mu$m, and $w = 5\ \mu$m. An additional resonant square structure with a gap (g) of 5 μm and a length ($leng\_out$) of 90 μm was attached to the outside of the SSLM. The attached square structure was close to and evenly apart from the SSLM to be directly and uniformly affected by the heat controlled by the SSLM as a micro-heater. When the DSLM was operated in mode 1, there were two abrupt changes of THz wave transmittance because of the dual-resonance of the DSLM. In addition, two strong resonances were observed in mode 2 because of the dual-resonance as shown in figure 2(c). Resonance at 0.71 THz mainly resulted from the size of the basic SSLM, and the other resonance at 0.30 THz resulted from the entire structure of the DSLM having the basic SSLM and additionally attached resonant structure. Thus, the stable band-pass characteristics could be realized between two strong resonances. The transmittance of the DSLM operating in mode 2 decreased from 85% to 0.3% at the peak of the passband, 0.47 THz, as the VO_2 conductivity increased from 20 to 1×10^6 S m^{-1}.

The surface currents of the DSLM operating in mode 2 at two different resonant frequencies are shown in figure 3. The surface current at the lower resonant frequency of 0.30 THz flowed through the whole structure of the DSLM, including the basic square-loop structure, the attached square structure, and the connection line between the two structures as shown in figure 3(a). The strength of the current was largely concentrated in the connection line. Conversely, the surface current at the higher resonant frequency of 0.71 THz flowed mostly through the basic square-loop structure and slightly through the inside part of the attached square structure as shown in figure 3(b). These indicate that the resonances at the lower and higher frequencies were mainly governed by the entire structure and the inner basic square-loop structure, respectively.

Single phase VO_2 thin films were grown on a single crystal Al_2O_3 (0001) substrate by using ion reactive radio-

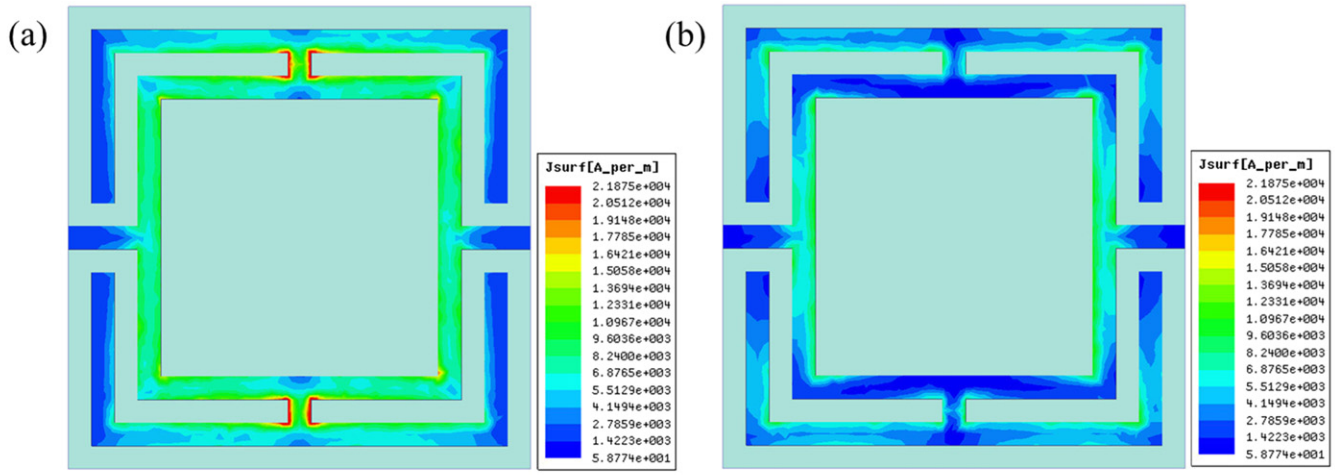

Figure 3. Simulation results for surface current density of dual-resonant square-loop metamaterial (DSLM) at resonant frequencies (a) 0.3 THz and (b) 0.71 THz.

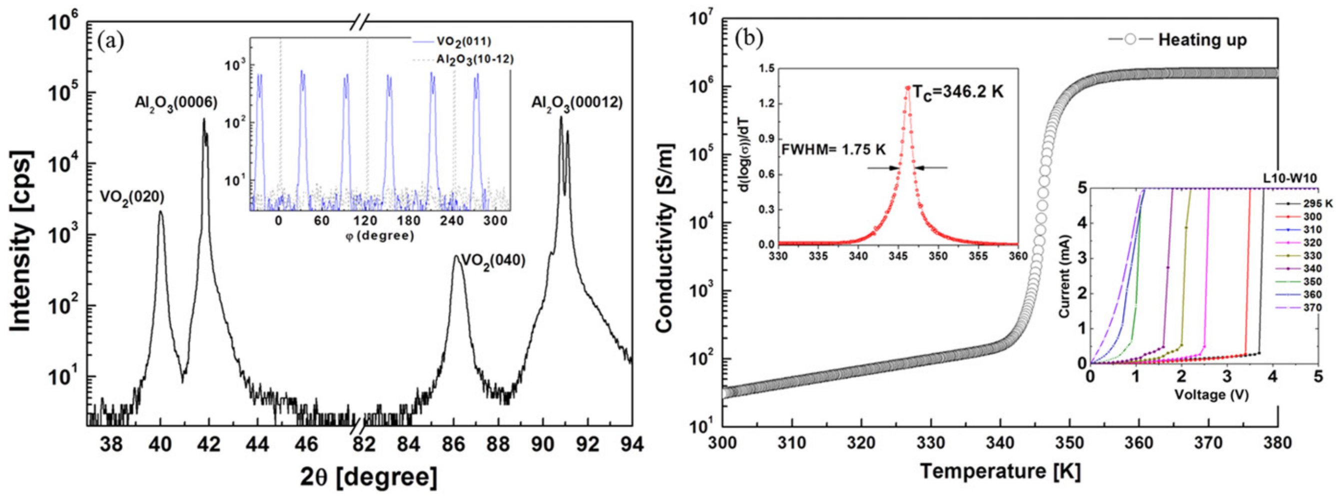

Figure 4. (a) Θ–2Θ x-ray diffraction pattern of the VO_2 thin film on Al_2O_3 (0001). (Inset: φ scan from 0° to 360° for the planes of VO_2 (011) and Al_2O_3 (10–12)). (b) Temperature dependence of electrical conductivity on the film. (Inset: 1st derivative of log(σ)-temperature and *I–V* curves at various temperatures for two-terminal device with channel dimension of 10×10 (μm^2)).

frequency (RF) sputtering. A 3 inch vanadium metal target with a purity of >99.99% was used for the film deposition, and the applied RF power and substrate temperature were maintained at 100 W and 550 °C, respectively, under a pressure of 5 mTorr. Throughout the growth process, a mixture of Ar and O_2 was introduced at fixed rates of 30 sccm and 0.03 sccm, respectively, within the vacuum chamber in which the sputtering process was performed. The grown films were spontaneously cooled to room temperature. The thickness of the VO_2 films was 100 nm, which was controlled by changing the deposition time and examined by a cross-sectional scanning electron microscope. The atomic spatial arrangement of the thin films in the out-of- and in-plane directions was measured by a θ–2θ scan and a φ scan in an x-ray diffractometer (RIGAKU, D/MAX-2500). Figure 4(a) shows the out-of-plane atomic displacement of the VO_2/Al_2O_3 (0001). In the x-ray diffraction measurement, Cu Kα radiation ($\lambda \sim 1.54$ Å) was used under an acceleration voltage of 40 kV and a current of 300 mA. Clear and sharp peaks of 2θ at approximately 40° and 86° correspond to monoclinic VO_2 (020) and (040) lattice plane spacing, respectively, indicating that the crystalline single phase VO_2 [010] domains are well-formed in parallel to Al_2O_3 [0001] direction. To investigate the in-plane epitaxial relation between VO_2 and Al_2O_3 (0001), a φ scan was performed from 0° to 360° for the planes of VO_2 (011) and Al_2O_3 (10–12) as shown in the inset of figure 4(a). From the observed results, the in-plane epitaxial relation can be determined as VO_2 (M) [100] or [001]|| $Al_2O_3\{11\bar{2}0\}$. Figure 4(b) shows a temperature dependence of electrical conductivity of the VO_2 thin film in an in-plane direction using four-probe measurement. The measured conductivity of the film showed a drastic change of about 5×10^4 (at $\sigma_{360K}/\sigma_{300K}$) near the transition temperature. From the measurement results, the conductivities are about 20 and 1×10^6 S m^{-1} at the insulator and metal phase, respectively, which are the start and end values used in the simulations. The left inset in figure 4(b) shows the detailed insulator-to-metal phase transition characteristics. The critical

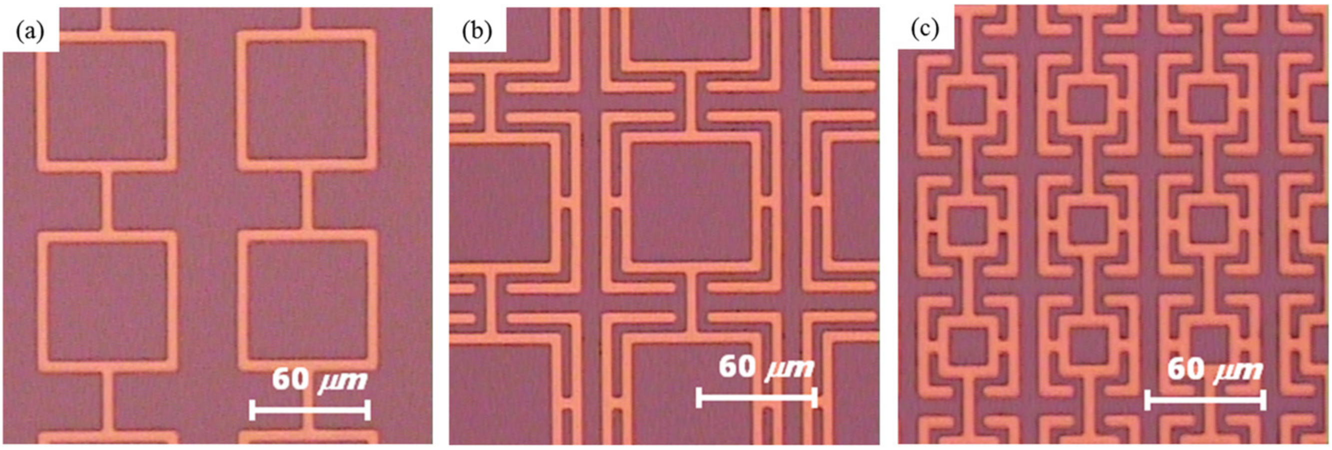

Figure 5. Photographs of the fabricated (a) SSLM, (b) DSLM, and (c) high-frequency dual-resonant square-loop metamaterial (HDSLM).

temperature (T_c), which is defined as the biggest value in the first-order derivative of log(σ)-temperature, was 346.2 K. The transition width of the phase transition—i.e., a full-width at half maximum, is only 1.75 K. These values indicate that the film quality is very high and comparable to the values of a single crystal [23]. Its sharp phase transition property is highly suitable for high-performance active devices. And *I–V* curves of the two-terminal device with VO_2 channel dimension of 10×10 (μm^2) were measured at various temperatures as shown in the right inset of figure 4(b).

The electrically tunable metamaterial based on VO_2 thin film was fabricated to prove that the proposed structure can possess the double functionalities of both a resonator and a micro-heater for the electrical control of the VO_2. A gold electrode (200 nm) with a Ti adhesion layer (20 nm) was deposited on top of the VO_2 thin film by the dc sputtering method. The designed metamaterials were patterned by using a general photolithography and a lift-off process. The photographs of the fabricated SSLM, DSLM, and high-frequency dual-resonant square-loop metamaterial (HDSLM) are presented in figure 5. The HDSLM is scaled-down version of the DSLM to be operated over 1.0 THz.

3. Experimental results and discussion

The designed and fabricated SSLM and DSLM were measured using THz time-domain spectroscopy (THz-TDS) system. In order to directly compare the performances of the SSLM and DSLM as micro-heaters with that of an external heater, the SSLM or DSLM was placed on the external heater, which had a hole in the center to facilitate good transmission of a THz wave. First, the transmittances of the SSLM and DSLM operating in an insulator phase of VO_2 thin film were measured (all OFF state—black lines in figures 6 and 7). Second, a bias voltage of 2 V was engaged in the SSLM and DSLM to increase the temperature and change the phase of the VO_2 from insulator to metal (micro-heater ON state—red lines in figures 6 and 7). Instead of the moderately varying characteristics of the device as shown in the simulation, only the ON and OFF states of the device were measured because the deposited VO_2 thin film showed the sharp phase transition property owing to its high quality. After measuring the transmittances of the SSLM and DSLM operating in a metal phase of VO_2, the bias voltages were turned off to return the VO_2 phase to insulator. Finally, the temperature of the external heater was increased to 360 K to change the phase of VO_2 from insulator to metal, and their transmittances were measured (external-heater ON state—blue lines in figures 6 and 7). Figure 6 presents the transmittances of the SSLM and DSLM while operating in insulator and metal phases of VO_2 thin film. The experimental results agree relatively well with those of the simulated results. The transmittances of the SSLM and DSLM operating in mode 1 show some ripples, which may result from the truncated signals in the time domain. Because the time-domain signals in mode 1 show long oscillation signals that are overlapped with the secondary internal-reflection signals inside the substrate with the metamaterial, the overlapped signals were truncated in the time domain for the fast Fourier transform. The measured resonance frequencies of the SSLM and DSLM in figure 6 were shifted to the lower frequencies compared with those of the simulated results. These differences could be caused by the deviation of the set simulation values from the real values of the material properties in the fabricated devices or the dimensions of the structures. When the metamaterials were operated in an insulator phase of VO_2 thin film, the transmittance of the SSLM in mode 2 was 1.2% at a resonance frequency of 0.56 THz; the transmittances of the DSLM were 4.7% and 1.85% at resonance frequencies of 0.27 THz and 0.65 THz, respectively. The transmittance of the DSLM (mode 2) operating in an insulator phase of VO_2 thin film was 77.8% at a frequency of 0.43 THz in the passband. The *Q*-factors of the DSLM operating in mode 2 were 2.22 at the center frequencies of 0.44 THz in the passband. Insets in figure 6 enlarge the transmittances of the SSLM and DSLM operating in metal phases of VO_2 thin films, which were heated by either a micro-heater (red-line) or an external heater (blue-line). These data show that the performances of the SSLM and DSLM as micro-heaters are the same as that of the

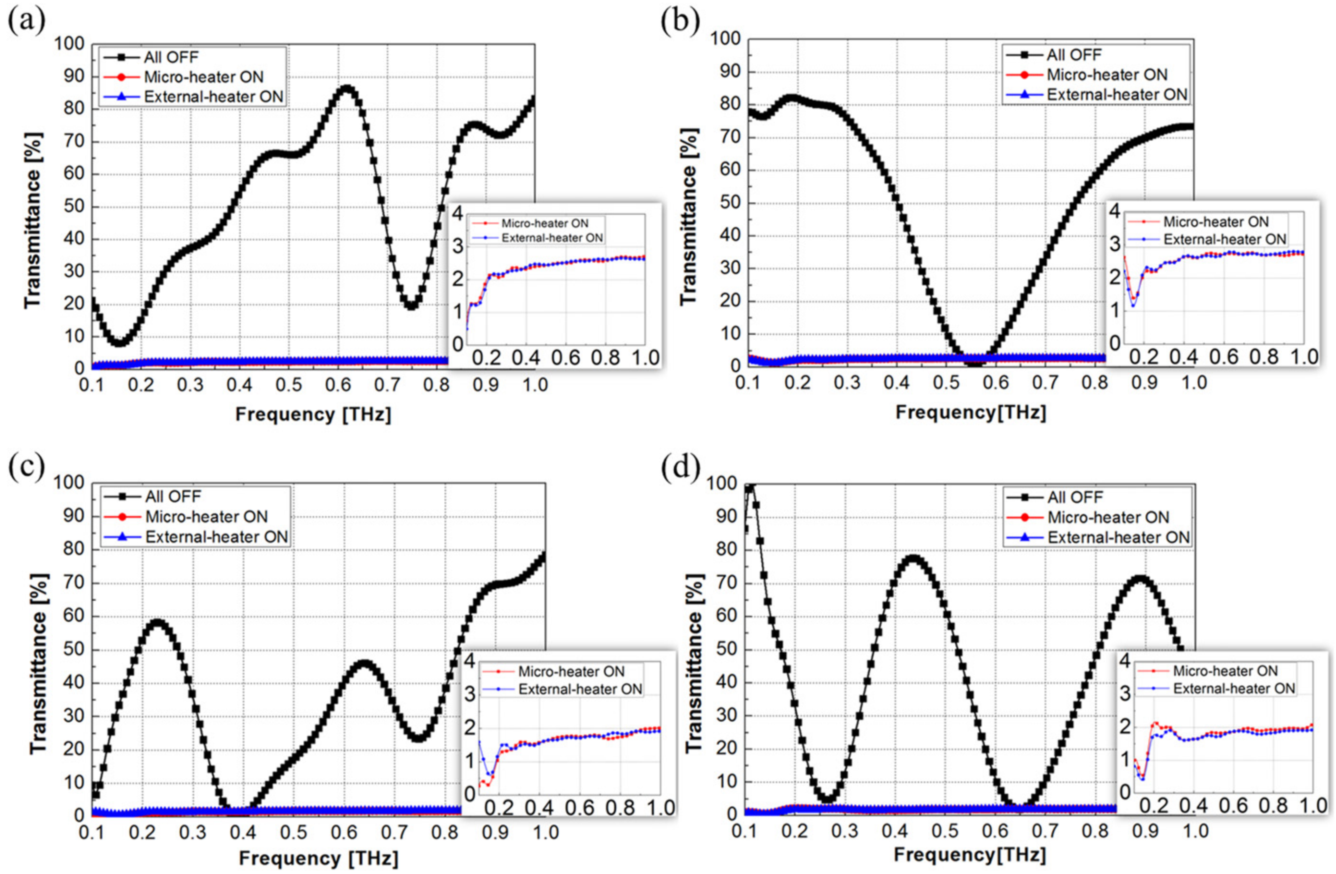

Figure 6. Measured transmittances of the SSLM and DSLM in an insulator and metal phases of VO_2 thin film (a) SSLM operating in mode 1, (b) SSLM operating in mode 2, (c) DSLM operating in mode 1, and (d) DSLM operating in mode 2. (Insets of figures 6(a)–(d): enlarged graphs for each comparison of ON state of micro-heater and external-heater).

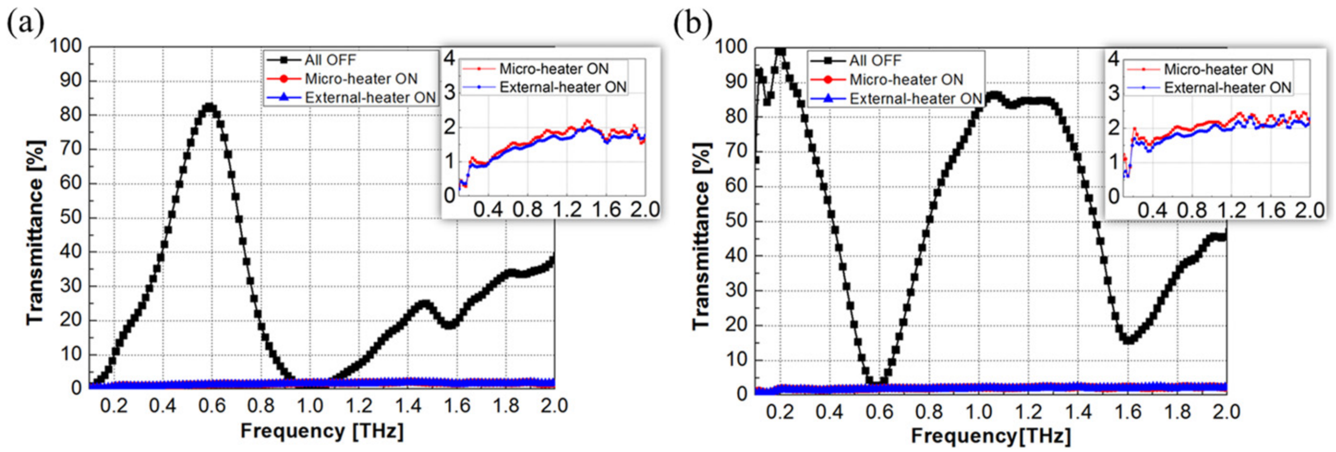

Figure 7. Measured transmittances of HDSLM in an insulator and a metal phase of VO_2 thin film (a) operating in mode 1 and (b) operating in mode 2. (Insets of figures 7(a) and (b): enlarged graphs for each comparison of ON state in micro-heater and external-heater).

external heater. The transmittances of the SSLM and DSLM operating in metal phases of VO_2 were less than 3% and 2%, respectively. The fabricated SSLM and DSLM successfully worked as both a resonator and a micro-heater.

The HDSLM was fabricated for operation in the frequency range over 1 THz. The width and gap of the HDSLM was fixed to 5 μm for easy fabrication by using a typical photolithography. The size of the HDSLM was scaled down from the DSLM to increase the operating passband frequency. The size of the unit cell and the dimensions of the HDSLM were $cell_w = 60\ \mu$m, $leng_out = 50\ \mu$m, $leng_in = 30\ \mu$m, $w = 5\ \mu$m, and $g = 5\ \mu$m as shown in figure 5(c). The HDSLM also worked well as both a micro-heater and a resonator. Figure 7 shows the measured transmittance of the HDSLM operating in modes 1 and 2. The transmittances of HDSLM in a metal phase of VO_2 were less than 2.5% in the

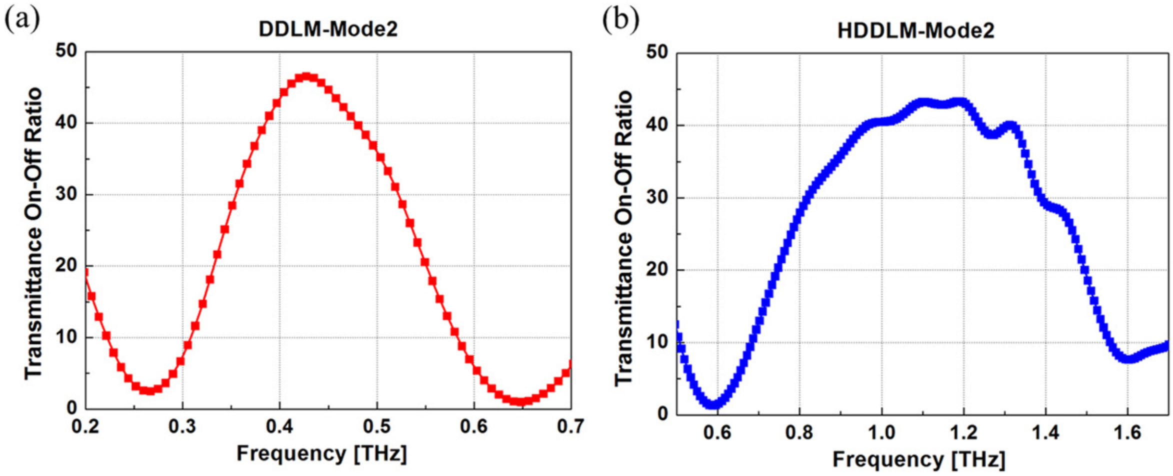

Figure 8. Transmittance on–off ratios of (a) the DSLM and (b) the HDSLM in mode 2.

entire frequency band from 0.1 to 2.0 THz. The transmittance of the HDSLM (mode 2) operating in an insulator phase of VO_2 thin film was 85% at a frequency of 1.27 THz in the passband. The Q-factors of the HDSLM operating in mode 2 were 1.61 at the center frequencies of 1.14 THz in the passband. The passband frequency range and the transmittance of the DSLM were successfully controlled by changing its dimensions and directly applying a bias voltage to it, respectively.

The DSLM and HDSLM operating in mode 2 could be used as an active THz filter by using the thermally induced phase transition characteristics of the VO_2 thin film. The phase transitions of the DSLM and HDSLM could be easily achieved by applying a bias voltage. The transmittance on–off ratios of the DSLM and HDSLM were 45 and 43 at the center frequencies of each passband, respectively, as shown in figure 8. These on–off switching characteristics of the proposed devices based on the undoped VO_2 thin film can be changed to the gradual switching characteristics by using W-doped VO_2 thin film which has wide tunable phase transition temperature range [24, 25]. Our measured results clearly show that the square-loop shaped metamaterial based on VO_2 thin film can be used as an active THz filters or sensors, which is easily controllable by a bias voltage.

4. Conclusion

We proposed an electrically controllable THz active metamaterial based on vanadium dioxide (VO_2) thin film. A square-loop shape was adopted to simultaneously perform roles as a resonating metamaterial and a micro-heater to electrically control the conductivity of the VO_2. Dual-resonant metamaterials were designed to realize band-pass characteristics in the desired operation frequency band. The measured electromagnetic properties of the metamaterials agreed relatively well with the simulated results. The measured Q-factors of the basic and scaled-down metamaterials fabricated on VO_2 thin films were 2.22 and 1.61 at the center frequencies of 0.44 THz and 1.14 THz, respectively. The transmittances of the active metamaterials based on VO_2 thin film were successfully controlled by directly applying a bias voltage instead of using an external heater. The measured transmittance on–off ratios of the metamaterials were over 40 at the center frequencies in the passbands. Our results clearly show the possibility of electrically controllable THz active devices based on VO_2 metamaterial. These easily controllable THz metamaterials can be used as high-performance active filters or sensors.

Acknowledgments

This research was supported by the Basic Science Research Program (grant no. 2013R1A1A1076113) through the National Research Foundation (NRF) of Korea and the Nano-Material Technology Development Program (grant no. 2012M3A7B4035095 and 2013M3A7B4054783).

References

[1] Jepsen P U, Cooke D G and Koch M 2011 Terahertz spectroscopy and imaging—modern techniques and applications *Laser Photon. Rev.* **5** 124–66
[2] Tonouchi M 2007 Cutting-edge terahertz technology *Nat. Photon.* **1** 97–105
[3] Liu H B, Zhong H, Karpowicz N, Chen Y and Zhang X C 2007 Terahertz spectroscopy and imaging for defense and security applications *Proc. IEEE* **95** 1514–27
[4] Han S-P *et al* 2012 Compact fiber-pigtailed InGaAs photoconductive antenna module for terahertz-wave generation and detection *Opt. Express* **20** 18432–9
[5] Ruy H-C, Kim N, Han S-P, Ko H, Park J-W, Moon K and Park K H 2012 Simple and cost-effective thickness measurement terahertz system based on a compact 1.55 μm $\lambda/4$ phase-shifted dual-mode laser *Opt. Express* **20** 25990–9
[6] Han S-P *et al* 2011 Optical fiber-coupled InGaAs-based terahertz time-domain spectroscopy system *Opt. Lett.* **36** 3094–6

[7] Boppel S *et al* 2012 CMOS integrated antenna-coupled field-effect transistors for the detection of radiation from 0.2 to 4.3 THz *IEEE Microw. Theory Tech.* **60** 3834–43
[8] Acuna G, Heucke S F, Kuchler F, Chen H-T, Tayler A J and Kersting R 2008 Surface plasmons in terahertz metamaterials *Opt. Express* **16** 18745–51
[9] Chen H-T, Padilla W J, Zide J M O, Gossard A C, Taylor A J and Averitt R D 2006 Active terahertz metamaterial devices *Nature* **444** 597–600
[10] Choi M, Lee S H, Kim Y, Kang S B, Shin J, Kwak M H, Kang K-Y, Lee Y-H, Park N and Min B 2011 A terahertz metamaterial with unnaturally high refractive index *Nature* **470** 369–73
[11] Chen H-T, Ohara J F, Azad A K, Taylor A J, Averitt R D, Shrekenhamer D B and Padilla W J 2008 Experimental demonstration of frequency-agile terahertz metamaterials *Nat. Photon.* **2** 295–8
[12] Jansen C, Al-Naib I A I, Born N and Koch M 2011 Terahertz metasurfaces with high *Q*-factors *Appl. Phys. Lett.* **98** 051109
[13] Chen H-T, Padilla W J, Cich M J, Azad A K and Averitt R D 2009 A metamaterial solid-state terahertz phase modulator *Nat. Photonics* **22** 148–51
[14] Ju L *et al* 2011 Graphene plasmonics for tunable terahertz metamaterials *Nat. Nanotechnol.* **4** 630–4
[15] Sensale-Rodriguez B, Yan R, Kelly M M, Fang T, Tahy K, Hwang W S, Jena D, Liu L and Xing H G 2012 Broadband graphene terahertz nodulators enabled by intraband transition *Nat. Commun.* **3** 1–7
[16] Wen Q-Y, Zhang H-W, Yang Q-H, Xie Y-S, Chen K and Liu Y-L 2010 Terahertz metamaterials with VO_2 cut-wires for thermal tunability *Appl. Phys. Lett.* **97** 021111
[17] Liu M *et al* 2012 Terahertz-field-induced insulator-to-metal transition in vanadium dioxide metamaterial *Nature* **487** 345–8
[18] Choi S B *et al* 2011 Nanopattern enabled terahertz all-optical switching on vanadium dioxide thin film *Appl. Phys. Lett.* **98** 071105
[19] Wen Q-Y, Zhang H-W, Chen Z, Long Y, Jing Y-L, Lin Y and Zhang P-X 2012 A tunable hybrid metamaterial absorber based on vanadium dioxide films *J. Phys. D: Appl. Phys.* **45** 235106
[20] Zhang Y, Qiao S, Sun L, Shi Q W, Huang W, Li L and Yang Z 2014 Photoinduced active terahertz metamaterials with nanostructured vanadium dioxide film deposited by sol-gel method *Opt. Express* **22** 11070–8
[21] Jeong Y G, Bernien H, Kyoung J S, Park H R, Kim H S, Choi J W, Kim B-J, Kim H–T, Ahn K J and Kim D S 2011 Electrical control of terahertz nano antennas on VO_2 thin film *Opt. Express* **19** 21211–5
[22] Ryu H-C 2014 Electrically controllable terahertz wave modulator based on a metamaterial and VO_2 thin film K *J. Opt. Phot.* **25** 279–85
[23] Berglund C N and Guggenheim H J 1969 Electronic properties of VO_2 near the semiconductor-metal transition *Phys. Rev.* **185** 1022–33
[24] Tan X *et al* 2012 Unraveling metal–insulator transition mechanism of VO_2 triggered by tungsten doping *Sci. Rep.* **2** 466
[25] Karaoglan-Bebek G, Hoque M N F, Holtz M, Fan Z and Bernussi A A 2014 Continuous tuning of W-doped VO_2 optical properties for terahertz analog applications *Appl. Phys. Lett.* **105** 201902